Molecular Dynamics Simulations of SOPS and Sphingomyelin Bilayers Containing Cholesterol

Shreyas Y. Bhide, Zhancheng Zhang, and Max L. Berkowitz
Department of Chemistry, University of North Carolina at Chapel Hill, Chapel Hill, North Carolina 27599

ABSTRACT   We performed a molecular dynamics simulation of an asymmetric bilayer that contained different lipid mixtures in its outer and inner leaflets. The outer leaflet contained a mixture of sphingomyelin (SM) with cholesterol and the inner leaflet a mixture of stearoyl-oleoyl-phosphatidylserine (SOPS) with cholesterol. For comparison purposes, we also performed two simulations on symmetric bilayers: the first simulation was performed on a bilayer containing a binary mixture of SOPS with cholesterol; the second contained a mixture of SM with cholesterol. We studied the hydrogen-bonding network of the bilayers in our simulations and the difference in the network properties in the monolayers either with SM or SOPS. We observed that in the asymmetric bilayer the properties of monolayers were the same as in the corresponding monolayers in the symmetric bilayers.

INTRODUCTION

Biological membranes are very complex entities containing many distinct lipid species (1). The distribution of these lipids in cell membranes is not homogeneous. Thus, for example, lipids such as sphingomyelin (SM) and phosphatidylcholine (PC) can be often found in the outer leaflet of plasma membranes, while two other typical lipids—phosphatidylserine (PS) and phosphatidylethanolamine—are found in the inner leaflet of the membrane (2,3). Another important lipid found in membranes is cholesterol (CHOL), but it is not known if it is distributed in the same amount in the two leaflets of the membrane (2). In view of the inhomogeneous character of natural membranes, it was proposed that these membranes contain domains where lipids exist in a liquid-ordered phase (L_o) surrounded by assemblies of lipids in the liquid-disordered phase (L_d) (4). The L_o domains are rich in cholesterol and saturated lipids; these domains are also often called lipid rafts (4,5). The issues related to our understanding of the composition, structure, dimensions, and properties of lipid rafts in natural biomembranes are very far from being clarified (6).

To study properties of lipid rafts, model membranes are intensely investigated. Numerous studies have been performed on bilayers containing binary mixtures of lipids with cholesterol as one of the components (7,8). Specifically, in view of the importance of the SM molecule for rafts, recent studies were done to understand the nature of interactions between SM and CHOL (9–11). Also, studies were done on model bilayers containing ternary mixtures of cholesterol, SM, and unsaturated PC and phase diagrams for these mixtures were mapped out (8,12). It was observed that in giant unilamellar vesicles containing the three components mentioned above, a phase separation occurs: the bilayers contain L_o domains (rafts) where CHOL and SM can be found in an enriched amount. The composition of both leaflets in model

systems was the same and it was observed that L_o domains were created simultaneously in both leaflets and the domains were in the same location in the inner and outer leaflets. What is the situation with the domains in natural membranes containing asymmetric (different in lipid composition) leaflets? As of today, no clear understanding of this issue exits (2).

Computer simulations of bilayers containing PC lipids or mixtures of PC with cholesterol provided molecular level information on structural and dynamical properties of such bilayers (13–18). Recently, results were reported on simulation studies done on SM bilayers (19–22) as well as on bilayers containing a binary mixture of SM and CHOL (23). Some preliminary, but thought-provoking simulation work was done on ternary mixtures containing dioleoylphosphatidylcholine, SM, and CHOL by Pandit et al. (24,25).

Nearly all simulations on bilayers containing lipid mixtures that were reported in the literature were performed on symmetric bilayers containing the same composition of both leaflets. In this work, we report a molecular dynamics (MD) simulation performed on an asymmetric bilayer containing a mixture of CHOL and (18:0) SM in one leaflet and stearoyl-oleoyl-phosphatidylserine (SOPS) and CHOL in the other leaflet. For comparison purposes, we also performed two simulations on symmetric bilayers: first simulation was performed on a bilayer containing a binary mixture of SOPS and CHOL (SOPS+CHOL), with the second containing a mixture of (18:0) SM and CHOL (SM+CHOL). We chose to simulate a mixture of PS molecules with CHOL because PS molecules interact more favorably with CHOL compared to phosphatidylethanolamine molecules (5). SOPS molecule is chosen to represent PS molecules, which are found in the cytoplasmic leaflet of natural membranes (26). The raft-forming concentration of cholesterol in the SM+CHOL bilayer was chosen for the study. Since the interaction between PS and CHOL is favorable and the PS molecules are condensed in the bilayer due to interlipid hydrogen-bonding interactions
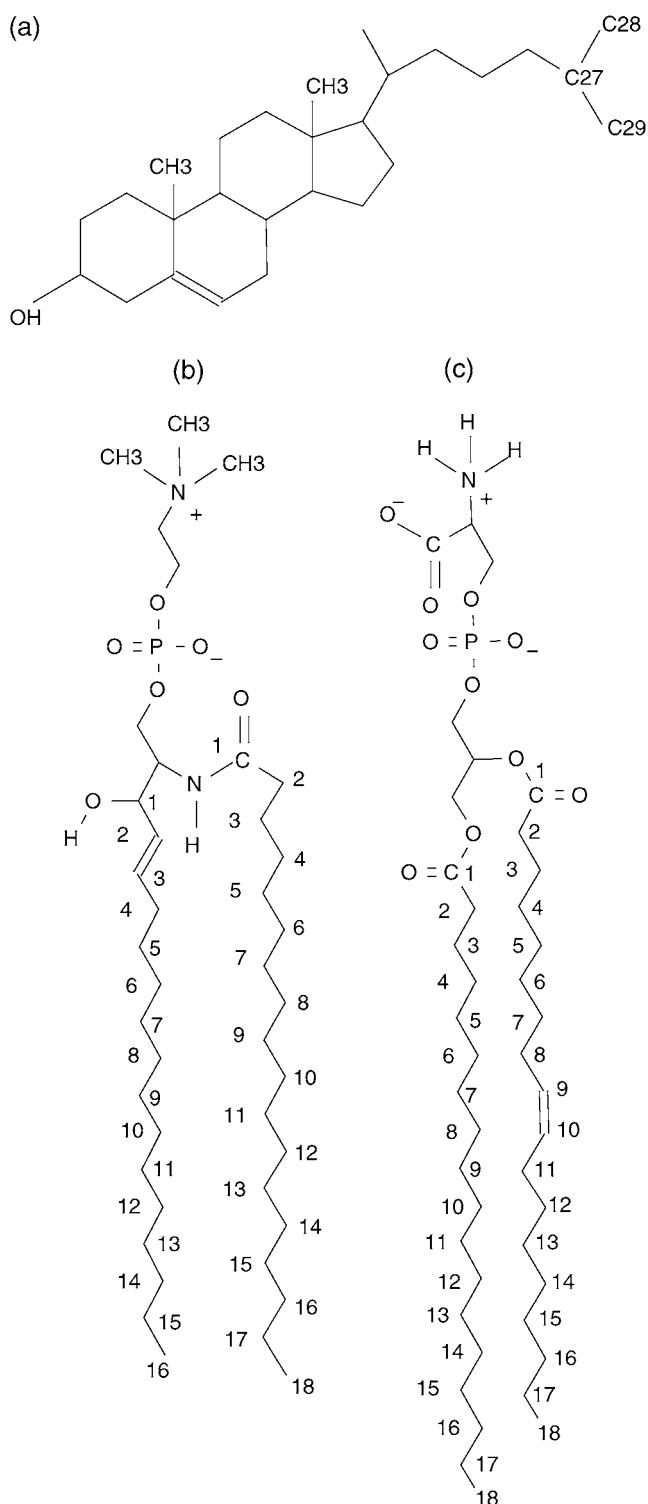
(a)

(b)   (c)

FIGURE 1   Structure of the lipid molecules (*a*) cholesterol (CHOL), (*b*) (18:0) sphingomyelin (SM), and (*c*) SOPS. The numbering is as used in the analyses.

and condensing effect due to counterions (27,28), we expect that the phase of the SOPS and CHOL mixture will also be the L_o phase. Therefore, we expect that in our simulation we represent a patch of an L_o domain in an asymmetric bilayer.

COMPUTATIONAL DETAILS

We have performed MD simulations on two symmetric bilayers containing mixtures of phospholipid molecules with cholesterol and one simulation on an asymmetric bilayer containing different mixtures in each leaflet. The first bilayer contained 84 SOPS molecules, 44 cholesterol (CHOL) molecules, and 84 Na^+ counterions. The second system had 84 (18:0) sphingomyelin (SM) molecules and 44 CHOL molecules. Both bilayers were hydrated with 3840 water molecules.

The molecular structures of SOPS (18:0), SM, and CHOL (see Fig. 1) were generated using SYBYL, Ver. 7.0 (Tripos, St. Louis, MO). The initial structure of a bilayer leaflet was obtained by generating an 8×8 array of 64 lipids (SOPS or (18:0) SM) in the *x,y* plane by random rotation of each lipid around the *z* direction. Then 22 of these phospholipids were
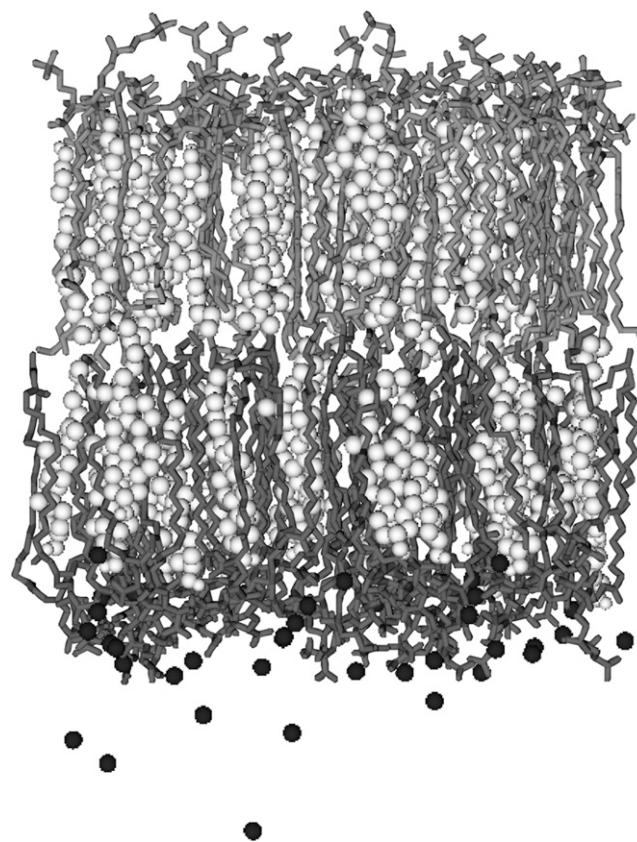

FIGURE 2   The asymmetric bilayer: SOPS (*solid-stick representation*), CHOL (*open spheres*), Na^+ (*solid spheres*) in the lower leaflet, SM (*shaded-stick representation*), and CHOL (*open spheres*) in the upper leaflet. The solvent water molecules are not shown.

randomly chosen and replaced by CHOL molecules. The second leaflet was obtained by reflection and translation of this first layer. A water slab was added on both sides to solvate the headgroups. In the case of SOPS bilayer, this was followed by a random replacement of 42 water molecules on each side of the bilayer by Na^+ ions. For both bilayers, the bilayer normal is directed along the z direction.

Our simulations were performed using the GROMACS package (29,30). The LINCS algorithm was used to constrain all bonds in the system (31) allowing an integration time step of 2 fs. Periodic boundary conditions were applied in all three dimensions and long-range electrostatics was handled using the SPME algorithm (32) with a real-space cutoff of 10 Å, fourth-order interpolation, and a tolerance of 10^{-5}. A 12 Å cutoff was utilized for van der Waals' interactions. The temperature in the simulations was maintained at 310 K using the Nosé-Hoover scheme (33) with a thermostat relaxation time of 0.5 ps. The system was simulated in an NPT ensemble using the Parrinello-Rahman semi-isotropic pressure-coupling scheme (34) with a barostat time constant of 2.0 ps at a pressure of 1 atm.

The SPC/E model of water (35) was used in the simulations. Force field for the SOPS was based on the parameters of Berger et al. (36) and the GROMOS87 (37) parameters. The

carboxylate group charges were taken from the aspartic acid side chain. The partial charges for amine group were the same as used in palmitoyl-oleoyl-phosphatidylcholine (38). The force field for the (18:0) SM was the same as used by Niemelä et al. (39). The force-field parameters of CHOL as used in the study by Pandit et al. (18) were also used in this study.

The SOPS and (18:0) SM bilayers were simulated for 60 ns and 64 ns, respectively. The positions and velocities of the system were saved after every 1 ps.

To construct the asymmetric bilayer we combined configurations of two lipid leaflets, each from the simulation with the symmetric SM+CHOL and SOPS+CHOL bilayers (see Fig. 2). The configurations were obtained from the end of 50 ns and 60 ns MD runs, respectively. Both leaflets contained 42 phospholipid and 22 CHOL molecules. In addition, the SOPS+CHOL leaflet contained 42 Na^+ counterions. A water slab of 1920 water molecules was generated using GROMACS utility genbox and added to each leaflet of the bilayer. The asymmetric bilayer structure was initially energy-minimized and then an MD simulation was carried out for 50 ns in an NPT ensemble at 1 atm pressure and at 310 K with the three-dimensional periodic boundary conditions. For the asymmetric bilayer, the force-field parameters and the simulation parameters were the same as described above for the symmetric bilayers. The trajectory data were saved every 1 ps.

The analyses of the saved data were performed using the utilities available in GROMACS as well as programs written
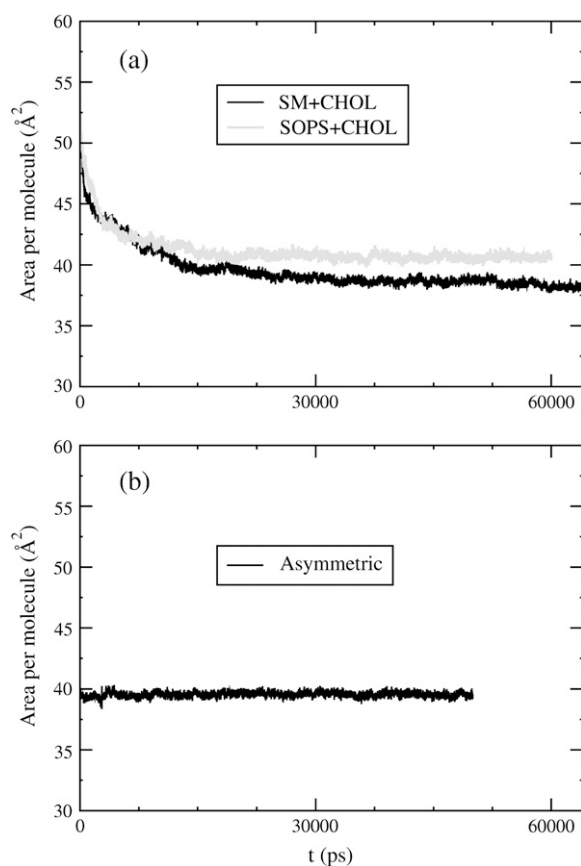

FIGURE 3 The area per molecule for (a) symmetric SOPS+CHOL and SM+CHOL bilayers and (b) asymmetric bilayer.
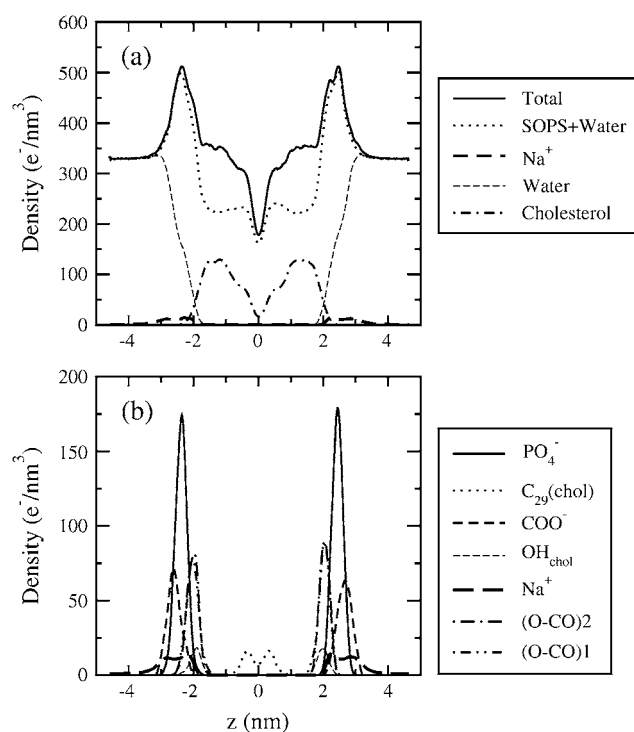

FIGURE 4 The electron density profile of the SOPS+CHOL bilayer plotted as a function of the distance along the bilayer normal.

by us. The analyses have been carried out over the last 45 ns and 38 ns of the trajectory for symmetric SOPS and (18:0) SM bilayers, respectively. For the asymmetric bilayer, the analyses were carried out over the last 45 ns of the trajectory. Henceforth, we refer to (18:0) sphingomyelin as SM, unless mentioned otherwise.

RESULTS AND DISCUSSION

Structural properties

Fig. 3 a shows the values for the areas per lipid from the two simulations performed on the symmetric bilayers. The values for the average area per lipid are 40.7 $\pm$ 0.3 and 38.6 $\pm$ 0.3 Å^2 for the bilayers containing SOPS and SM phospholipids, respectively. These numbers seem to be somewhat small, when compared to areas per lipid of ~50–70 Å^2 measured in monolayers or bilayers containing only one lipid component (40). Since we have cholesterol molecules in our bilayers, the area condenses. That the numbers given above are reasonable can be understood from the following argument. Let us assume that cholesterol is shielded from water by phospholipids, as it is suggested in the umbrella model (41). In this case one gets that the area per phospholipid is $a_{PL} = A/N_{PL}$, where a_{PL} is the area per headgroup of the phospholipid (SOPS or SM), A is the xy area of the simulation box, and N_{PL} is the number of phos-

pholipids. From the umbrella model one gets for phospholipids area values of 62 Å^2 for SOPS and 58.8 Å^2 for SM. The value for SOPS is close to the measured value of $\approx$64 Å^2 obtained for dioleoyl-phosphatidylserine (42). It is expected that the area per SOPS should be substantially smaller than the one for dioleoyl-phosphatidylserine, because SOPS contains only one unsaturated bond. The area per SM as estimated above is also larger than the area per SM of ~51 Å^2 obtained from simulations on pure SM bilayer (39). These considerations indicate that the umbrella model is probably not accurate for area estimates. Getting the values for areas per lipid in simulations with lipid mixtures is not a simple issue (43). Here we have used the methodology developed by Hofsäß et al. (17) to compare our data with some of the data published in the literature for the cholesterol/dipalmitoylphosphatidylcholine (DPPC) mixture. According to Hofsäß et al., the areas per phospholipid and cholesterol can be determined using the equation

$$a_{PL} = \frac{2A}{(1-x)N_{lipid}}\left[1 - \frac{xN_{lipid}V_{chol}}{V - N_w V_w}\right],$$

where N_{lipid} is the total number of lipids ($N_{PL} + N_{CHOL} = 128$), x is N_{CHOL}/N_{lipid}, V is the volume of the simulation box, N_w is the total number of water molecules in the system, V_w is the volume occupied per water molecule (0.0305 nm^3), and V_{chol} is the volume per cholesterol molecule taken to be 0.593 nm^3 (17). The area per cholesterol molecule can be calculated from the expression
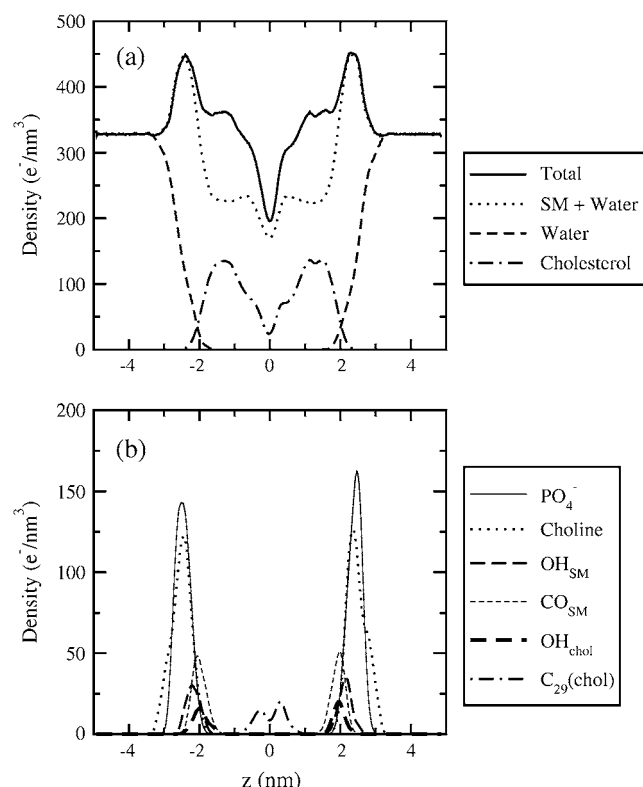

FIGURE 5 The electron density profile of the SM+CHOL bilayer plotted as a function of the distance along the bilayer normal.
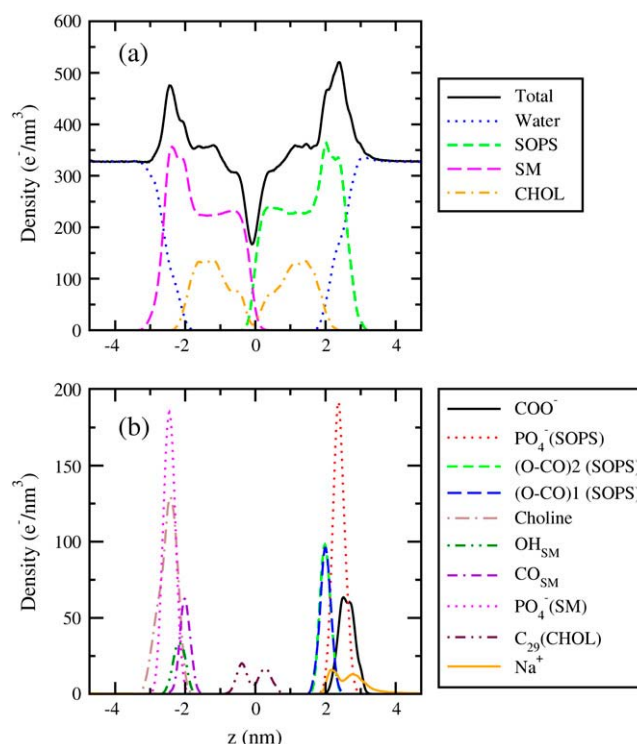

FIGURE 6 The electron density profile of the asymmetric bilayer plotted as a function of the distance along the bilayer normal.

$$a_{\mathrm{chol}} = \frac{2A - a_{\mathrm{PL}} N_{\mathrm{PL}}}{N_{\mathrm{chol}}}.$$

The calculated values of area per lipid using the above equations are $a_{\mathrm{SOPS}} = 48.8$ Å^2 and $a_{\mathrm{SM}} = 46.3$ Å^2. The area per cholesterol is 25 Å^2 in both systems. For comparison, notice that in the DPPC+CHOL bilayer containing 40% cholesterol, the DPPC area is ~55 Å^2, while the CHOL area is ~27 Å^2 (17). So, when 40% of cholesterol is added to DPPC, its area in simulations shrinks from 64 Å^2 to ~55 Å^2, while the area of SM shrinks from ~51 Å^2 to ~46 Å^2 when we add 33% of cholesterol. This indicates that in membranes containing PC a substantial condensation occurs with the addition of cholesterol. Some condensation also occurs in membranes containing SM, but this condensation is not as substantial. The bilayer of pure SM is already condensed due to the presence of a strong interlipid hydrogen-bonding network. The same can be also argued about the bilayers containing PS.

Fig. 3 b shows the time evolution of the area per lipid in the asymmetric bilayer. The average area per lipid molecule is 39.5 ± 0.2 Å^2 in this case. To find the area per lipid in case of the asymmetric bilayer we observed that the xy area of the simulation box for the asymmetric bilayer is the same for the

two leaflets and that both leaflets have the same number of phospholipid and cholesterol molecules. Therefore, from the above-described procedure for calculating areas, if one assumes that the area/cholesterol is the same in two leaflets, one obtains that the area/phospholipid is also the same for the two types of phospholipids. The area/phospholipid is found to be 47.4 Å^2 and the area/cholesterol is ≈25 Å^2. Thus, the area/phospholipid in the asymmetric bilayer is intermediate to the values of the area/SOPS and the area/SM as found above.

Fig. 4, a and b, shows the electron density plots for the SOPS+CHOL system. The peak-to-peak distance, as estimated from Fig. 4 a, is found to be 48.2 Å. When compared to the experimental measurement of bilayer thickness ≈42 Å of pure SOPS bilayer (44), the SOPS+CHOL bilayer in the present work appears to be more extended. From Fig. 4 b, it can be seen that Na$^+$ ions are delocalized over the bilayer water interface. The ions are located in the region stretching from the carboxylate group to the ester-carbonyl groups denoted as (O-CO)1 for the sn-1 chain and (O-CO)2 for the sn-2 chain. No significant overlap of densities in the z direction is observed between hydroxyl groups of cholesterol and the Na$^+$ ions. However, the hydroxyl groups of cholesterol are seen to be in the proximity of ester-carbonyl groups of SOPS.
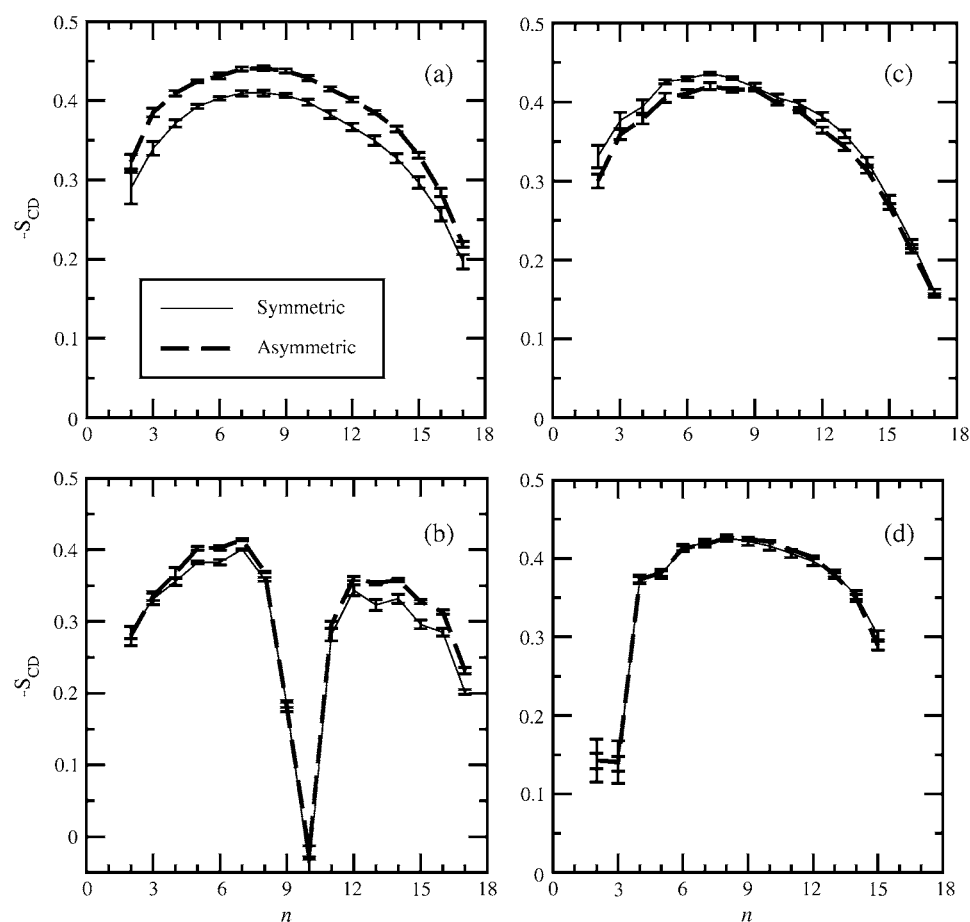

FIGURE 7 Deuterium order parameter profiles for symmetric and asymmetric bilayers. (a) Stearoyl and (b) oleoyl chains of SOPS. (c) Stearoyl and (d) sphingosine chain of SM. n is the number of carbon atoms along the hydrocarbon chains as shown in Fig. 1.

The electron density of the tail CH_3 group of cholesterol shows very little overlap across the bilayer. This can be seen as a consequence of the presence of an 18-carbon tails in the SOPS molecules.

Fig. 5, *a* and *b*, shows the electron density plot of the SM+CHOL system. The peak-to-peak distance in Fig. 5 *a* is found to be 47.6 Å. Khelashvili and Scott (23) also performed simulations of an 18:0 SM with cholesterol in a proportion which was roughly 2:1. Their areas per lipids were ~10% larger than reported here and correspondingly

their peak-to-peak distance was significantly shorter (42 Å). Note that the force field and the simulation temperatures were different in the simulations of Khelashvili and Scott. As in the case of SOPS bilayer, we did not observe any significant overlap of the tail methyl group densities (C_{29}) of cholesterol molecules in the case of the SM+CHOL bilayer (see Fig. 5 *b*). At the same time, the density of the hydroxyl group of cholesterol is found to have a significant overlap with the densities of the CO and –OH groups of the SM molecules.
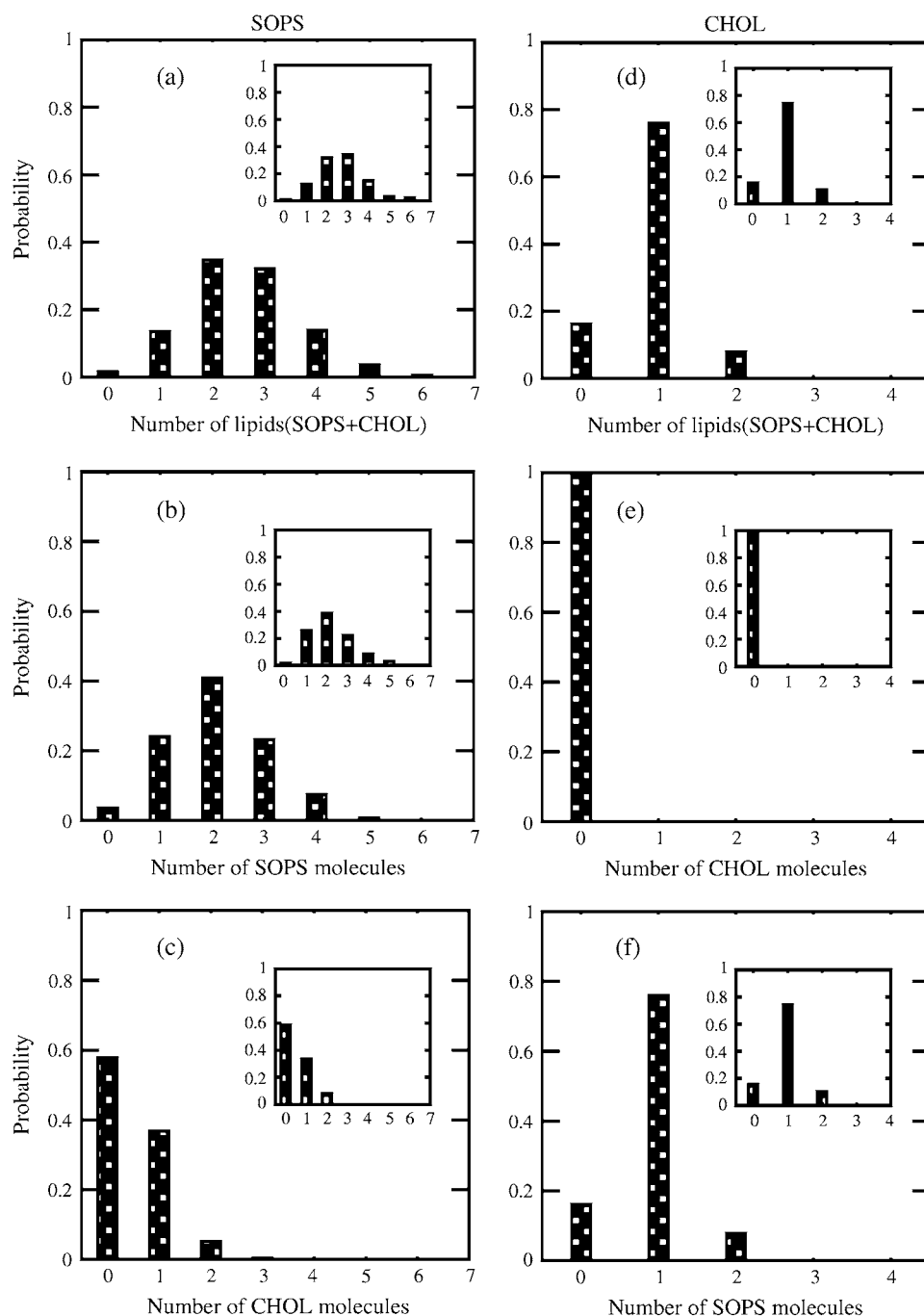

FIGURE 8 Distribution of molecules that are hydrogen-bonded to a given lipid in SOPS+CHOL bilayer. Distribution of (*a*) total number of lipids, (*b*) total number of SOPS molecules, and (*c*) total number of cholesterol molecules that are hydrogen-bonded to a given SOPS molecule. Panels *d–f* show the distribution of total number of lipids, total number of cholesterol molecules, and total number of SOPS molecules, respectively, that are hydrogen-bonded to a given cholesterol molecule. Inset in each plot shows the corresponding distribution of molecules that are hydrogen-bonded to a given lipid in the SOPS+CHOL leaflet of the asymmetric bilayer.

Fig. 6, *a* and *b*, shows the electron density profiles for the asymmetric bilayer. The peak-to-peak distance in Fig. 6 *a* is found to be 48.4 Å. The Na^+ ions were found to be located only on the side of the SOPS+CHOL leaflet, despite the presence of the three-dimensional periodic boundary conditions. These ions were delocalized over the interfacial region from carboxylate to the ester-carbonyl groups. As in the symmetric bilayers, tail groups C_{29} of CHOL were found to have a minimal overlap in the asymmetric bilayer (Fig. 6 *b*).

We also calculated the deuterium-order parameter (45) profiles for the lipid chains. These are shown in Fig. 7. The

order parameters for the lipid chains in the symmetric bilayers indicate that the sphingosine and the stearoyl chains of SM are slightly more ordered than the stearoyl chain of SOPS. Fig. 7, *a* and *b*, shows that the effect of the bilayer asymmetrization in our simulation was most significant for the SOPS+CHOL leaflet. The stearoyl chain and, to some extent the oleoyl chain, of the SOPS became more ordered in the asymmetric bilayer than in the symmetric bilayer. The ordering of the sphingosine chain of SM remained unaffected by the asymmetrization (Fig. 7 *d*), while the stearoyl chain became slightly less ordered (Fig. 7 *c*). Thus, for the
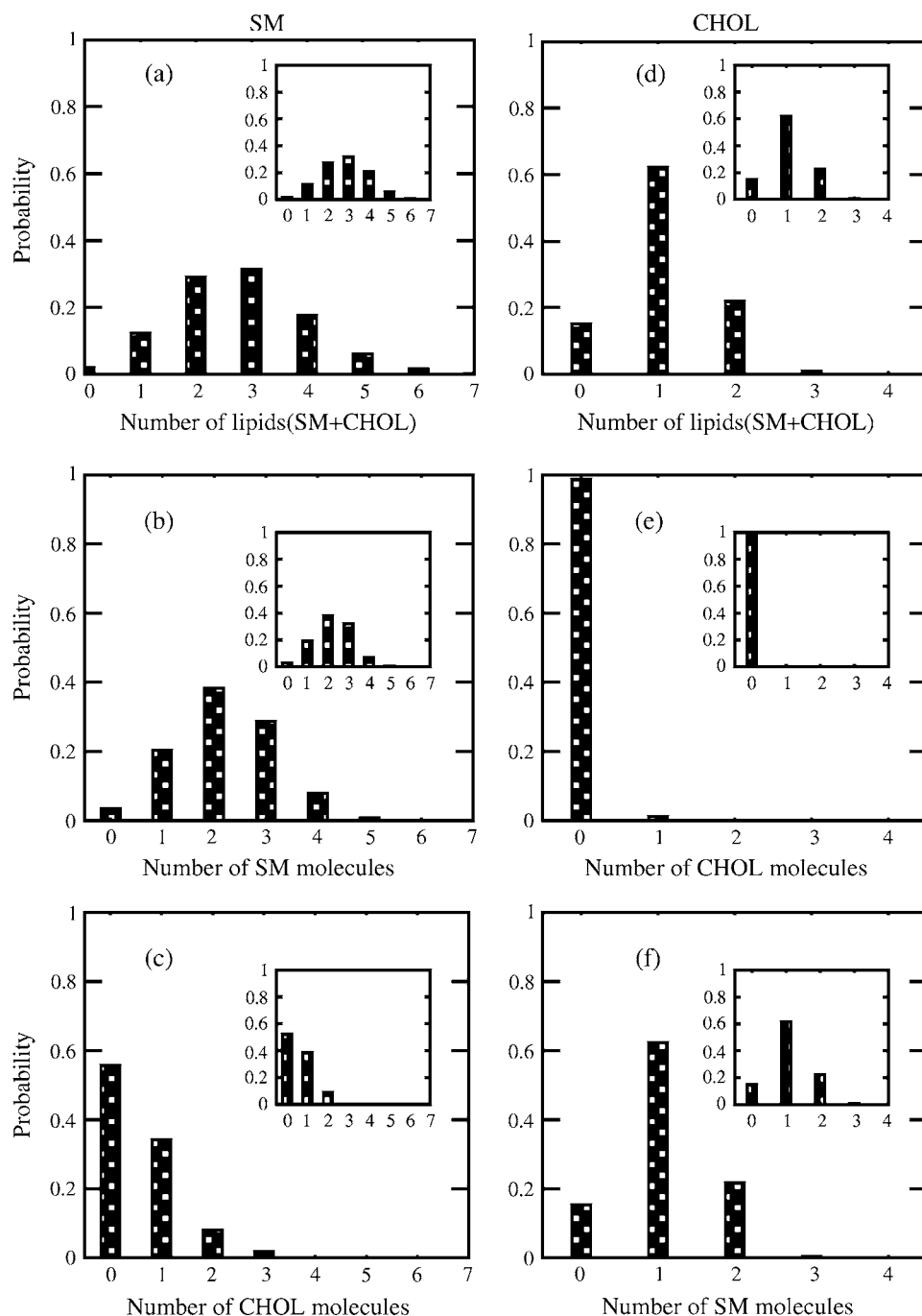

FIGURE 9 Distribution of molecules that are hydrogen-bonded to a given lipid in SM+CHOL bilayer. Distribution of (*a*) total number of lipids, (*b*) total number of SM molecules, and (*c*) total number of cholesterol molecules that are hydrogen-bonded to a given SM molecule. Panels *d–f* show the distribution of total number of lipids, total number of cholesterol molecules, and total number of SM molecules, respectively, that are hydrogen-bonded to a given cholesterol molecule. Inset in each plot shows the corresponding distribution of molecules that are hydrogen-bonded to a given lipid in the SM+CHOL leaflet of the asymmetric bilayer.

symmetric bilayers, the SM+CHOL bilayer exhibits a lower average area/molecule and therefore a larger lipid chain order than the SOPS+CHOL bilayer. In the asymmetric bilayer, the SOPS+CHOL leaflet gets more ordered while the order in the SM+CHOL leaflet slightly decreases as compared to the symmetric bilayer. This is consistent with the observed trend of area/lipid (see Fig. 3).

The results of our simulations on symmetric bilayers demonstrate that geometrical parameters such as areas per lipid and chain order parameters (for saturated bonds) are very close in cases of SOPS+CHOL and SM+CHOL bilayers. Does this mean that if the SM+CHOL bilayer phase is the L_o phase, the phase of the SOPS+CHOL bilayer is also an L_o phase and that SOPS and CHOL mixture is also raft-forming? If we follow a previously proposed suggestion that raft-forming tendencies are connected to cholesterol-lipid complex-forming tendencies (46), and these in turn are correlated with hydrogen-bonding network properties (18) we need to study properties of hydrogen bonding networks in our bilayers.

Properties of hydrogen-bonding network

Let us consider here the interlipid hydrogen-bonding properties of the bilayers. We use the geometric criteria for the definition of the hydrogen bond between two lipids. To this end, for SOPS+CHOL bilayer, a radial distribution function was calculated between hydrogen atoms of groups such as NH_3^+ of SOPS and $-OH$ of CHOL and the oxygen atoms belonging to different molecules in the system. The first minima for these radial distribution functions was found to be $\sim$2.5 Å. Therefore, an interlipid hydrogen bond was assumed to exist when the distance between a hydrogen atom from one lipid and an oxygen atom from the other lipid, r_{HO} is <2.5 Å and the angle hydrogen–donor–oxygen, θ_{HDO}, is <30°. In the present work, the donor can either be a nitrogen or an oxygen atom. This definition of hydrogen bond is similar to the criterion used by Mukhopadhyay et al. (47), who had used $r_{HO} \leq 2.4$ Å and $\theta_{HDO} \leq 35°$. In the case of the pure SM bilayer, it was shown recently (22) that among -OH and -NH groups only the -NH group participates in the interlipid hydrogen bond. In addition to the definition of the hydrogen bond given above, to study the interlipid hydrogen bonding in the SM+CHOL mixture, we assume that the hydrogen bond can be made between the $N^+(CH_3)_3$ group of the SM and the OH group of cholesterol. The existence of such a bond was proposed when interlipid hydrogen bonding was studied for the bilayer containing dipalmitoylphosphatidylcholine (DPPC) and cholesterol mixture (18). The concept of CH⋯O hydrogen bond is well established in
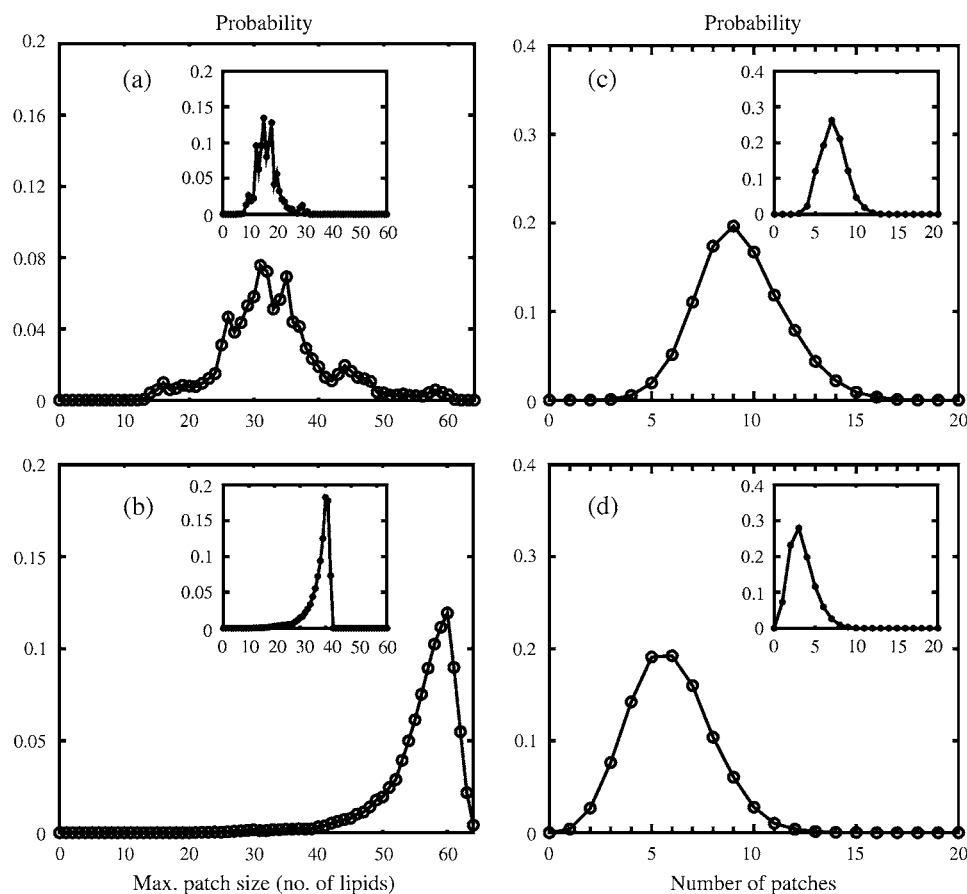
FIGURE 10 The distribution of maximum patch size in a leaflet of (*a*) SOPS+CHOL and (*b*) SM+CHOL bilayer. Patch size is measured in terms of the number of lipids that constitute the patch. The distribution of the number of patches in a leaflet of (*c*) SOPS+CHOL and (*d*) SM+CHOL bilayer. Calculation takes into account all types of interlipid bonding. Inset of each plot shows the corresponding distribution calculated using interlipid bonding among phospholipids only. In each plot the line is drawn as a guide to the eye only.

chemistry (48–51). The geometric criterion used for identifying this interlipid hydrogen bond for the united-atom model of CH_3 was also used in the earlier work on lipid complexation (28). The hydrogen bond between $N^+(CH_3)_3$ and $-OH_{CHOL}$ is assumed to exist whenever the distance between CH_3 group and oxygen is <4 Å and the angle between N–CH_3–O is in the range between 79° and 139°. This criterion is also used to identify hydrogen-bonding interaction between the two charged groups, $N^+(CH_3)_3$ and PO_4^-, belonging to two different SM molecules.

Fig. 8 shows the distributions of the number of molecules hydrogen-bonded to a given lipid in the SOPS+CHOL bilayer. As we can see from Fig. 8 a, an SOPS molecule has a maximum probability to be hydrogen-bonded with two other lipids, which according to Fig. 8 b will be, with a high probability, two SOPS molecules. Also, an SOPS molecule is most likely not to be hydrogen-bonded to a cholesterol, as cholesterol concentration is ~33% (see Fig. 8 c). In addition, SOPS is not found to be hydrogen-bonded to more than two cholesterol molecules. The distribution for the total number of hydrogen bonds per cholesterol is dominated by the presence of just one hydrogen bond between the SOPS molecule and cholesterol (see Fig. 8, d and f). Notice also the absence of the cholesterol-cholesterol hydrogen bonding.

Fig. 9 shows the distribution of a number of molecules that are hydrogen-bonded to a lipid in the SM+CHOL bilayer. As in the case of SOPS+CHOL bilayer, the distribution of number of lipids hydrogen-bonded to cholesterol is dominated by the corresponding distribution of SM molecules hydrogen-bonded to cholesterol, while the probability for the cholesterol-cholesterol hydrogen bonding is insignificant (see Fig. 9, d–f). While the distribution of hydrogen bonds for the SOPS molecule was peaked at two hydrogen bonds, the peak of the distribution for the SM molecule is at three hydrogen bonds. Both SM-cholesterol and SM-SM hydrogen-bonding make a contribution into the total distribution (see Fig. 9, a–c). Also, for the SM+CHOL bilayer, a cholesterol molecule has a higher probability of participating in a hydrogen bonding with two phospholipids, if compared to the case of the SOPS+CHOL bilayer (see Figs. 8 f and 9 f).

Insets in Figs. 8 and 9 show the distributions of molecules hydrogen-bonded to a given lipid in the two leaflets of the asymmetric bilayer. While the distribution of hydrogen bonds per SOPS molecule is peaked at two bonds for the symmetric bilayer, it is peaked at three in the asymmetric bilayer. As the comparison of plots in Fig. 8 shows, the difference comes from a subtle change in the bonding character of SOPS with other lipids in the bilayer. Properties of the distributions for the number of lipid molecules hydrogen-bonded to a given cholesterol molecule in the SOPS+CHOL leaflet remain the same as in the case of the symmetric SOPS+CHOL bilayer. The shift of the most probable number of hydrogen bonds for the SOPS+CHOL leaflet is consistent with the increase of order observed from calculations on area and order parameters when going from the symmetric to asymmetric bilayer.

The properties of the distributions of hydrogen-bonded molecules in case of SM+CHOL leaflet of the asymmetric bilayer are similar to those in the symmetric SM+CHOL bilayer (see Fig. 9). This is also consistent with our previous observations on order parameters (Fig. 7).

From the histograms shown in Figs. 8 and 9 we conclude that individual cholesterol molecules are more prone to engage in hydrogen-bonding with SM molecules compared to PS molecules. To understand the collective properties of the interlipid hydrogen-bond network we perform an analysis of hydrogen-bonded patches or clusters formed in each bilayer leaflet. A patch is defined as a group of lipids that share at least one hydrogen bond among them. The patch size is reported in terms of the number of lipids that constitute a patch. Fig. 10 shows the results for the upper leaflet of the two bilayers, the results for the lower leaflets are the same, since the bilayers are symmetrical. For the SM + CHOL

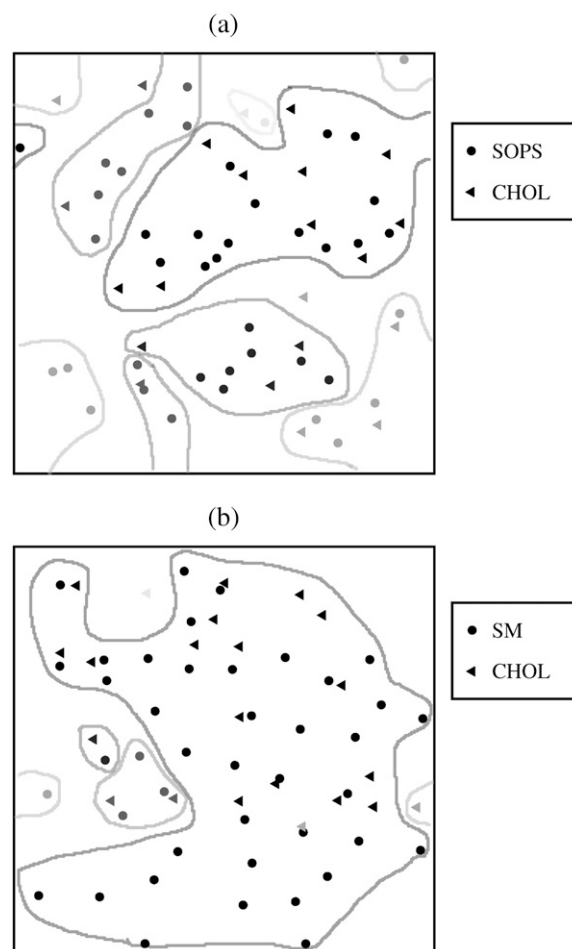FIGURE 11   A schematic view of the different patch sizes in a leaflet of (*a*) SOPS+CHOL bilayer and (*b*) SM+CHOL bilayer. The solid circles represent positions in the *x,y* plane of nitrogen atoms from NH_3^+ of SOPS and $N^+(CH_3)_3$ of SM, while the triangles represent the positions in the *x,y* plane of the oxygen atoms of CHOL. The line around the patches is drawn only as a guide to the eye.

bilayer, the direct bonding between charge groups like $N^+(CH_3)_3$ and PO_4^- is also taken into account. Fig. 10, a and b, shows the distributions of maximum number of lipids contained in a patch for the SOPS+CHOL and SM+CHOL bilayers, respectively. These distributions were obtained from the trajectories and therefore they characterize the dynamics of the hydrogen bonding. As we see from Fig. 10 a the most probable patch contains maximum of ~30 lipids in case of the SOPS+CHOL bilayer. For the SM+CHOL bilayer the most probable patch contains ~60 lipids maximum, as Fig. 10 b shows. This is close to the situation when the whole leaflet in our simulation box is connected through the network of hydrogen bonds. Distributions for the number of distinct patches in a leaflet, shown in Fig. 10, c and d, indicate the level of organization or fragmentation of the bilayer surface. It can be seen from Fig. 10 that the SOPS+CHOL bilayer surface is more fragmented than the SM+CHOL bilayer surface. These properties of network of interlipid bonding or patches were calculated for all types of interlipid bonding. It is important to know the contribution of the phospholipid (PL) + CHOL hydrogen bonding to the overall patch size. This can be investigated by identifying the interlipid bonding network only due to PL molecules. The corresponding results are shown as an inset in Fig. 10. As can be seen from the inset to Fig. 10, a and b, the influence of

cholesterol on the patch size is different for the SOPS+CHOL and SM+CHOL bilayers. For the SM+CHOL bilayer, the most probable patch contains maximum of ~40 SM molecules. This number is close to the total number of SM molecules in the leaflet. For the SOPS+CHOL bilayer, the distribution shows that most probable patches contain between 15 and 20 phospholipids. The number of distinct SM patches is also smaller than the average number of distinct SOPS patches (see *inset* to Fig. 10, c and d). As we saw previously any given cholesterol molecule is most likely to be hydrogen-bonded to a single phospholipid molecule rather than to two or more phospholipid molecules (see Figs. 8 f and 9 f). The consequences of this are manifested on a nanoscale through the results on patch sizes shown in Fig. 10. Based on data from Figs. 8–10, we conclude that a cholesterol molecule does not act as a bridge between two patches to form a large patch that can cover nearly the whole leaflet. Rather cholesterol increases the size of the patch mostly by just connecting through hydrogen bonds to the patch that exists because of hydrogen-bonding between phospholipids. Fig. 11, a and b, shows a schematic of patches of different sizes that exist in leaflets of SOPS+CHOL and SM+CHOL bilayers, respectively. In Fig. 11, a and b, positions of nitrogen atoms from the NH_3^+ group of SOPS and the $N^+(CH_3)_3$ group of SM and the position of oxygen atoms
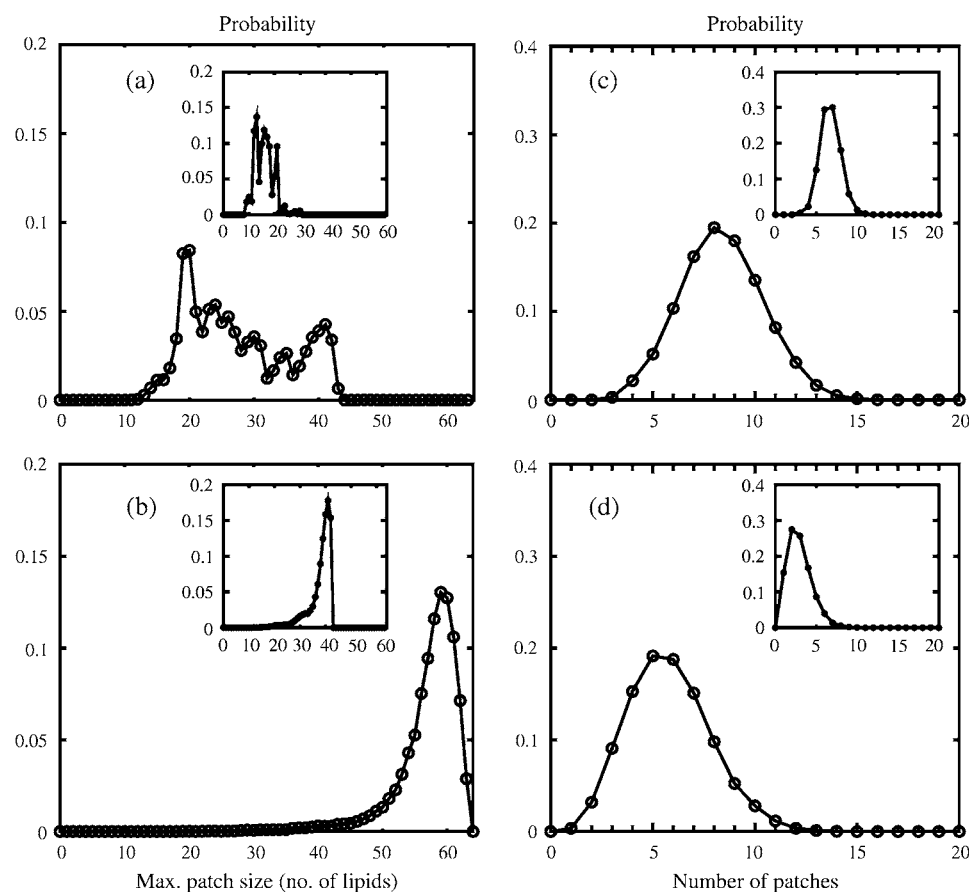

FIGURE 12 The distribution of maximum patch size in (a) SOPS+CHOL leaflet and (b) SM+CHOL leaflet of the asymmetric bilayer. Patch size is measured in terms of the number of lipids that constitute the patch. The distribution of the number of patches in (c) SOPS+CHOL leaflet and (d) SM+CHOL leaflet of the asymmetric bilayer. Calculation takes into account all types of interlipid bonding. Inset of each plot shows the corresponding distribution calculated using interlipid bonding among phospholipids only. In each plot the line is drawn as a guide to the eye only.

from CHOL are plotted in the *x,y* plane as representative of respective lipids.

Fig. 12 shows the distributions of hydrogen-bond network patches for the asymmetric bilayer when the PL-CHOL hydrogen-bonding is taken into account. Insets to Fig. 12 show the distributions calculated by considering only the phospholipid hydrogen-bond network. As can be seen from Fig. 12, the average properties of the patch sizes did not undergo a significant change by going from the symmetric to the asymmetric bilayer. Thus we conclude that the interleaflet coupling in the asymmetric bilayer did not induce any large-scale changes in the surface organization of the two leaflets as compared to the symmetric bilayers.

CONCLUSION

The histograms from Figs. 8 and 9 demonstrate that in the symmetric SM+CHOL and SOPS+CHOL bilayers the individual lipid molecules have nearly the same number of hydrogen-bonded nearest neighbors, although some slight differences between Figs. 8 and 9 exist. These differences practically disappear from the histograms shown in insets to Figs. 8 and 9, meaning that the hydrogen bonding per lipid is the same in the asymmetric bilayer. Nevertheless, as Figs. 10–12 show, the hydrogen-bonding network is different for the two symmetric bilayers with the SM+CHOL bilayer having more robust and SOPS+CHOL bilayer having more fractured characters. If one correlates the robustness of hydrogen-bonded network with the tendency to create L_o domains, one concludes that in the SM+CHOL mixtures the probability to observe rafts on a larger spatial scale is higher. From the simulations performed on the asymmetric bilayers we conclude that properties of the monolayers in the leaflets (with compositions specific for our simulations), do not change much when going from a symmetric to an asymmetric bilayer, indicating that cross-leaflet interactions such as interdigitations are unimportant. The outer leaflet in an asymmetric bilayer (containing SM+CHOL) is more prone for raft creation compared to the inner leaflet.

The conclusions from our simulations are consistent with the ideas expressed in the work of Devaux and Morris (2), who proposed that the sizes of the L_o domains in membrane leaflets should not be the same and that, possibly, proteins may play an important role in creation and functioning of rafts.

Finally, we would like to mention that although our simulations were performed on relatively long timescales for simulations (tens of nanoseconds), the large-scale rearrangements of lipids are not possible on this timescale. Nevertheless, if the cross-leaflet interaction would be important, we would observe its effects on the timescale of our simulation.

REFERENCES

1. Katsaras, J., and T. Gutberlet, editors. 2001. Lipid Bilayers: Structure and Interactions. Springer Verlag, Berlin.

2. Devaux, P. F., and R. Morris. 2004. Transmembrane asymmetry and lateral domains in biological membranes. *Traffic.* 5:241–246.

3. Nelson, D. L., and M. M. Cox. 2005. Lehninger: Principles of Biochemistry, 4th Ed. W. H. Freeman and Company, New York.

4. Simons, K., and E. Ikonen. 1997. Functional rafts in cell membranes. *Nature.* 387:569–572.

5. Simons, K., and W. L. C. Vaz. 2004. Model systems, lipid rafts, and cell membranes. *Annu. Rev. Biophys. Biomol. Struct.* 33:269–295.

6. Hancock, J. F. 2006. Lipid rafts: contentious only from simplistic standpoints. *Nat. Rev. Mol. Cell Biol.* 7:456–462.

7. McMullen, T. P. W., and R. N. McElhaney. 1996. Physical studies of cholesterol-phospholipid interactions. *Curr. Opin. Colloid Interface Sci.* 1:83–90.

8. Veatch, S. L., and S. L. Keller. 2005. Seeing spots: complex phase behavior in simple membranes. *Biochim. Biophys. Acta Mol. Cell Res.* 1746:172–185.

9. Holopainen, J. M., A. J. Metso, J. P. Mattila, A. Jutila, and P. K. J. Kinnunen. 2004. Evidence for the lack of a specific interaction between cholesterol and sphingomyelin. *Biophys. J.* 86:1510–1520.

10. Térová, B., R. Heczko, and J. P. Slotte. 2005. On the importance of the phosphocholine methyl groups for sphingomyelin/cholesterol interactions in membranes: a study with ceramide phosphoethanolamine. *Biophys. J.* 88:2661–2669.

11. Filippov, A., G. Orädd, and G. Lindblom. 2006. Sphingomyelin structure influences the lateral diffusion and raft formation in lipid bilayers. *Biophys. J.* 90:2086–2092.

12. de Almeida, R. F., A. Fedorov, and M. Prieto. 2003. Sphingomyelin-phosphatidylcholine-cholesterol phase diagram: boundaries and composition of lipid rafts. *Biophys. J.* 85:2406–2416.

13. Tu, K., M. L. Klein, and D. J. Tobias. 1998. Constant-pressure molecular dynamics investigation of cholesterol effects in a dipalmitoylphosphatidylcholine bilayer. *Biophys. J.* 75:2147–2156.

14. Smondyrev, A. M., and M. L. Berkowitz. 1999. Structure of dipalmitoylphosphatidylcholine/cholesterol bilayer at low and high cholesterol concentrations: molecular dynamics simulation. *Biophys. J.* 77:2075–2089.

15. Róg, T., and M. Pasenkiewicz-Gierula. 2001. Cholesterol effects on the phosphatidylcholine bilayer nonpolar region: a molecular simulation study. *Biophys. J.* 81:2190–2202.

16. Chiu, S. W., E. Jakobsson, R. J. Mashl, and H. L. Scott. 2002. Cholesterol-induced modifications in lipid bilayers: a simulation study. *Biophys. J.* 83:1842–1853.

17. Hofsäß, C., E. Lindahl, and O. Edholm. 2003. Molecular dynamics simulations of phospholipid bilayers with cholesterol. *Biophys. J.* 84:2192–2206.

18. Pandit, S. A., D. L. Bostick, and M. L. Berkowitz. 2004. Complexation of phosphatidylcholine lipids with cholesterol. *Biophys. J.* 86:1345–1356.

19. Chiu, S. W., S. Vasudevan, E. Jakobsson, R. J. Mashl, and H. L. Scott. 2003. Structure of sphingomyelin bilayers: A simulation study. *Biophys. J.* 85:3624–3635.

20. Hyvonen, M. T., and P. T. Kovanen. 2003. Molecular dynamics simulation of sphingomyelin bilayer. *J. Phys. Chem. B.* 107:9102–9108.

21. Mombelli, E., R. Morris, W. Taylor, and F. Fraternali. 2003. Hydrogen bonding propensities of sphingomyelin in solution and in a bilayer assembly: a molecular dynamics study. *Biophys. J.* 84:1507–1517.

22. Niemelä, P. S., M. T. Hyvönen, and I. Vattulainen. 2004. Structure and dynamics of sphingomyelin bilayer: insight gained through systematic comparison with phosphatidylcholine. *Biophys. J.* 87:2976–2989.

23. Khelashvili, G. A., and H. L. Scott. 2004. Combined Monte Carlo and molecular dynamics simulation of hydrated 18:0 sphingomyelin-cholesterol lipid bilayers. *J. Chem. Phys.* 120:9841–9847.

24. Pandit, S. A., E. Jacobsson, and H. L. Scott. 2004. Simulation of the early stages of nano-domain formation in mixed bilayers of sphingomyelin, cholesterol and dioleoylphosphatidylcholine. *Biophys. J.* 87:3312–3322.

25. Pandit, S. A., S. Vasudevan, S. W. Chiu, R. J. Mashl, E. Jacobsson, and H. L. Scott. 2004. Sphingomyelin-cholesterol domains in phospholipid membrane: atomistic simulation. *Biophys. J.* 87:1092–1100.

26. Fridriksson, E. K., P. A. Shipkova, E. D. Sheets, D. Holowka, B. Baird, and F. W. McLafferty. 1999. Quantitative analysis of phospholipids in functionally important membrane domains from RBL-2H3 mast cells using tandem high resolution mass spectrometry. *Biochemistry.* 38:8056–8063.

27. Pandit, S. A., and M. L. Berkowitz. 2002. Molecular dynamics simulation of dipalmitoylphosphatidylserine bilayer with Na$^+$ counterions. *Biophys. J.* 82:1818–1827.

28. Pandit, S. A., D. Bostick, and M. L. Berkowitz. 2003. Mixed bilayer containing dipalmitoylphosphatidylcholine and dipalmitoylphosphatidylserine: lipid complexation, ion binding, and electrostatics. *Biophys. J.* 85:3120–3131.

29. Berendsen, H. J. C., D. van der Spoel, and R. van Drunen. 1995. GROMACS: a message-passing parallel molecular dynamics implementation. *Comput. Phys. Comm.* 91:43–56.

30. Lindahl, E., B. Hess, and D. van der Spoel. 2001. GROMACS 3.0: a package for molecular simulation and trajectory analysis. *J. Mol. Mod.* 7:306–317.

31. Hess, B., H. Bekker, H. J. C. Berendsen, and J. G. E. M. Fraaige. 1997. LINCS: a linear constraint solver for molecular simulations. *J. Comput. Chem.* 18:1463–1472.

32. Essmann, U., L. Perera, M. L. Berkowitz, T. Darden, H. Lee, and L. G. Pedersen. 1995. A smooth particle mesh Ewald method. *J. Chem. Phys.* 103:8577–8593.

33. Nose, S., and M. L. Klein. 1983. Constant pressure molecular dynamics for molecular systems. *Mol. Phys.* 50:1055–1076.

34. Parrinello, M., and A. Rahman. 1981. Polymorphic transitions in single crystals: a new molecular dynamics method. *J. Appl. Phys.* 52:7182–7190.

35. Berendsen, H., J. R. Grigera, and T. P. Straatsma. 1987. The missing term in effective pair potentials. *J. Phys. Chem.* 91:6269–6271.

36. Berger, O., O. Edholm, and F. Jahnig. 1997. Molecular dynamics simulations of a fluid bilayer of dipalmitoylphosphatidylcholine at full hydration, constant pressure, and constant temperature. *Biophys. J.* 72:2002–2013.

37. van Gunsteren, W. F., A. A. Billeter, A. A. Eising, P. H. Hünenberger, P. Krüuger, A. E. Mark, W. R. P. Scott, and I. G. Tironi. 1996. Biomolecular Simulation: the GROMOS96 Manual and User Guide. Vdf Hochschulverlag AG and der ETH, Zürich, Switzerland.

38. Tieleman, D. P., and H. J. C. Berendsen. 1998. A molecular dynamics study of the pores formed by *Escherichia coli* OmpF porin in a fully hydrated palmitoyloleoylphosphatidylcholine bilayer. *Biophys. J.* 74:2786–2801.

39. Niemelä, P. S., M. T. Hyvönen, and I. Vattulainen. 2006. Influence of chain length and unsaturation on sphingomyelin bilayers. *Biophys. J.* 90:851–863.

40. Nagle, J. F., and S. Tristram-Nagle. 2000. Structure of lipid bilayers. *Biochim. Biophys. Acta Rev. Biomembr.* 1469:159–195.

41. Huang, J., and G. W. Feigenson. 1999. A microscopic interaction model of maximum solubility of cholesterol in lipid bilayers. *Biophys. J.* 76:2142–2157.

42. Petrache, H. I., S. Tristram-Nagle, K. Gawrisch, D. Harries, V. A. Parsegian, and J. F. Nagle. 2004. Structure and fluctuations of charged phosphatidylserine bilayers in the absence of salt. *Biophys. J.* 86:1574–1586.

43. Edholm, O., and J. F. Nagle. 2005. Areas of molecules in membranes consisting of mixtures. *Biophys. J.* 89:1827–1832.

44. Brzustowicz, M. R., and A. T. Brunger. 2005. X-ray scattering of unilamellar lipid vesicles. *J. Appl. Crystallogr.* 38:126–131.

45. Douliez, J.-P., A. Léonard, and E. J. Dufourc. 1995. Restatement of order parameters in biomembranes: calculation of C–C bond order parameters for C-D quadrupolar splittings. *Biophys. J.* 68:1727–1739.

46. McConnell, H. M., and A. Radhakrishnan. 2003. Condensed complexes of cholesterol and phospholipids. *Biochim. Biophys. Acta.* 1610:159–173.

47. Mukhopadhyay, P., L. Monticelli, and D. P. Tieleman. 2004. Molecular dynamics simulation of palmitoyl-oleoyl phosphatidylserine bilayer with Na$^+$ counterions and NaCl. *Biophys. J.* 86:1601–1609.

48. Desiraju, G. R. 1991. The C–H···O hydrogen bond in crystals: what is it? *Acc. Chem. Res.* 24:290–296.

49. Jeffrey, G. A. 1997. An Introduction to Hydrogen Bonding. Oxford University Press, New York.

50. Gu, Y., T. Kar, and S. Scheiner. 1999. Fundamental properties of the CH···O interaction: is it a true hydrogen bond? *J. Am. Chem. Soc.* 121:9411–9422.

51. Raveendran, P., and S. L. Wallen. 2002. Cooperative C–H···O hydrogen bonding in CO_2–Lewis base complexes: implications for solvation in supercritical CO_2. *J. Am. Chem. Soc.* 124:12590–12599.